Article

Cell Stem Cell

Inflammation-Induced Emergency Megakaryopoiesis Driven by Hematopoietic Stem Cell-like Megakaryocyte Progenitors

Graphical Abstract

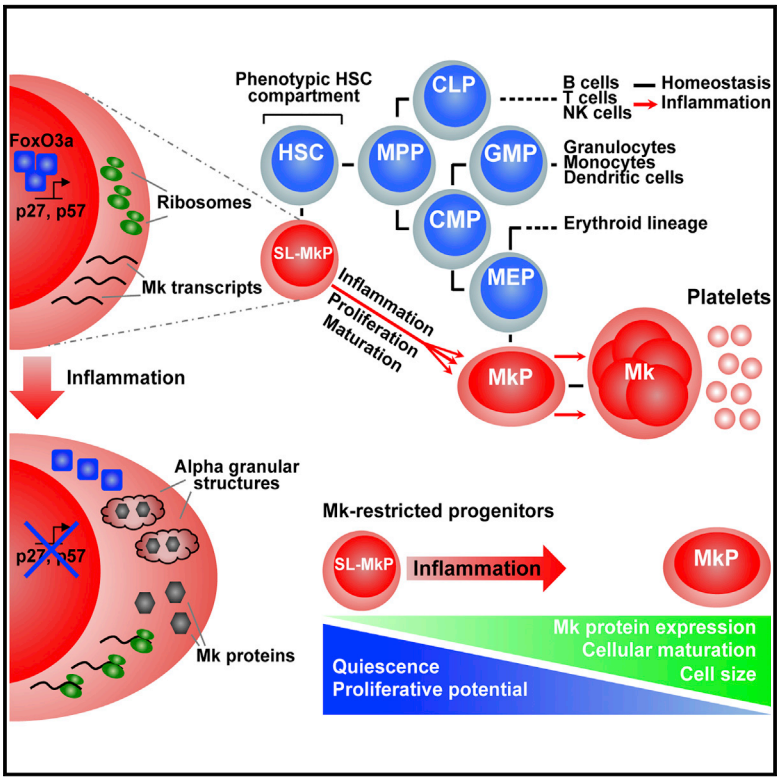

Highlights

- Unipotent SL-MkPs are maintained in a quiescent, but primed, state during homeostasis
- Inflammation instructs post-transcriptional Mk protein synthesis in SL-MkPs
- Inflammation drives efficient cell cycle activation and maturation of SL-MkPs
- Activation of SL-MkPs rapidly replenishes the platelet pool during acute inflammation

Authors

Simon Haas, Jenny Hansson, Daniel Klimmeck, ..., Andreas Trumpp, Jeroen Krijgsveld, Marieke A.G. Essers

Correspondence

m.essers@dkfz.de

In Brief

Haas et al. show that inflammatory signaling activates post-transcriptional protein synthesis, maturation, and cell cycle induction in quiescent, but primed, stem-like megakaryocyte progenitors. This emergency program efficiently prevents otherwise life-threatening platelet depletion during acute inflammation.

Accession Numbers

GSE64002

Haas et al., 2015, Cell Stem Cell *17*, 422–434
October 1, 2015
http://dx.doi.org/10.1016/j.stem.2015.07.007

CellPress

Cell Stem Cell
Article

Inflammation-Induced Emergency Megakaryopoiesis Driven by Hematopoietic Stem Cell-like Megakaryocyte Progenitors

Simon Haas,[1,2] Jenny Hansson,[3,13] Daniel Klimmeck,[1,3,4] Dirk Loeffler,[5] Lars Velten,[3] Hannah Uckelmann,[1,2] Stephan Wurzer,[1,2] Áine M. Prendergast,[1,2] Alexandra Schnell,[1,2] Klaus Hexel,[6] Rachel Santarella-Mellwig,[7] Sandra Blaszkiewicz,[1,2] Andrea Kuck,[1,2] Hartmut Geiger,[8,9] Michael D. Milsom,[1,10] Lars M. Steinmetz,[3,11,12] Timm Schroeder,[5] Andreas Trumpp,[1,4] Jeroen Krijgsveld,[3] and Marieke A.G. Essers[1,2,*]

[1]Heidelberg Institute for Stem Cell Technology and Experimental Medicine (HI-STEM gGmbH), 69120 Heidelberg, Germany
[2]Division of Stem Cells and Cancer, Hematopoietic Stem Cells and Stress Group, Deutsches Krebsforschungszentrum (DKFZ), 69120 Heidelberg, Germany
[3]European Molecular Biology Laboratory (EMBL), Genome Biology Unit, 69117 Heidelberg, Germany
[4]Division of Stem Cells and Cancer, Deutsches Krebsforschungszentrum (DKFZ), 69120 Heidelberg, Germany
[5]Department of Biosystems Science and Engineering (D-BSSE), ETH Zurich, 4058 Basel, Switzerland
[6]Core Facility Flow Cytometry, Deutsches Krebsforschungszentrum (DKFZ), 69120 Heidelberg, Germany
[7]European Molecular Biology Laboratory (EMBL), Electron Microscopy Core Facility, 69117 Heidelberg, Germany
[8]Institute for Molecular Medicine, Ulm University, 89081 Ulm, Germany
[9]Division of Experimental Hematology and Cancer Biology, Cincinnati Children's Hospital Medical Center and University of Cincinnati, Cincinnati, OH 45229, USA
[10]Division of Stem Cells and Cancer, Experimental Hematology Group, Deutsches Krebsforschungszentrum (DKFZ), 69120 Heidelberg, Germany
[11]Stanford Genome Technology Center, Palo Alto, CA 94304, USA
[12]Department of Genetics, Stanford University School of Medicine, Stanford, CA 94305, USA
[13]Present address: Division of Molecular Hematology, Lund Stem Cell Center, Lund University, 221 84 Lund, Sweden
*Correspondence: m.essers@dkfz.de
http://dx.doi.org/10.1016/j.stem.2015.07.007

SUMMARY

Infections are associated with extensive platelet consumption, representing a high risk for health. However, the mechanism coordinating the rapid regeneration of the platelet pool during such stress conditions remains unclear. Here, we report that the phenotypic hematopoietic stem cell (HSC) compartment contains stem-like megakaryocyte-committed progenitors (SL-MkPs), a cell population that shares many features with multipotent HSCs and serves as a lineage-restricted emergency pool for inflammatory insults. During homeostasis, SL-MkPs are maintained in a primed but quiescent state, thus contributing little to steady-state megakaryopoiesis. Even though lineage-specific megakaryocyte transcripts are expressed, protein synthesis is suppressed. In response to acute inflammation, SL-MkPs become activated, resulting in megakaryocyte protein production from pre-existing transcripts and a maturation of SL-MkPs and other megakaryocyte progenitors. This results in an efficient replenishment of platelets that are lost during inflammatory insult. Thus, our study reveals an emergency machinery that counteracts life-threatening platelet depletions during acute inflammation.

INTRODUCTION

The continuous production of blood and immune cells is regulated by a small number of multipotent and self-renewing hematopoietic stem cells (HSCs) residing in the bone marrow of adult mammals (Orkin and Zon, 2008). In response to bone marrow injury or infection, long-term quiescent HSCs are efficiently recruited into the cell cycle and return back to quiescence after re-establishment of homeostasis (Baldridge et al., 2010; Essers et al., 2009; Wilson et al., 2008). Positioned at the apex of the hierarchically organized hematopoietic system, HSCs generate a series of progenitor cells that undergo several consecutive commitment steps, becoming progressively restricted in their lineage potential and finally producing unipotent progenitors (Orkin and Zon, 2008). Megakaryocytes (Mks) are large, polyploid cells that release platelets into the circulation (Machlus and Italiano, 2013). According to the classical model of hematopoiesis, each mature Mk derives from an HSC that sequentially transitioned through the multipotent progenitor (MPP), common myeloid progenitor (CMP), Mk-erythroid progenitor (MEP), and Mk progenitor (MkP) states, followed by endomitosis to generate a mature Mk (Machlus and Italiano, 2013). However, the first evidence for a potential bypass of some intermediate states from HSCs toward Mks was provided when transcriptional profiling revealed expression of Mk transcripts in highly purified HSCs (Månsson et al., 2007). More recently, mRNA expression of the Mk marker von Willebrand factor (*Vwf*) and the surface receptor c-Kit were suggested to be indicative of a platelet-biased, but multipotent

HSC sub-population (Sanjuan-Pla et al., 2013; Shin et al., 2014). Moreover, the existence of Mk-lineage restricted cells with high self-renewal activity in the phenotypic HSC compartment was proposed based on single-cell transplantation experiments (Yamamoto et al., 2013). However, a molecular and cellular characterization of these potent Mk-restricted cells is lacking and the purpose of Mk-lineage priming effects and potential physiological benefits of shortcuts into the Mk lineage remain unclear.

Recent reports highlight the importance of platelets as inflammatory and immune cells in addition to their well-known function in thrombosis (Semple et al., 2011; Yeaman, 2014). Systemic inflammation associated with acute infections triggers the release of immunomodulatory agents and the interaction of platelets with neutrophils to facilitate the formation of neutrophil extracellular traps (NETs) (Jenne et al., 2013; Yeaman, 2014). This provokes a rapid consumption of platelets, resulting in a transient thrombocytopenia (Stohlawetz et al., 1999; Tacchini-Cottier et al., 1998). During acute inflammation, low platelet levels are associated with a loss of vascular integrity and hemorrhage, as well as septic shock, resulting in increased mortality (Goerge et al., 2008; Xiang et al., 2013). Therefore, a fast recovery of platelet levels is essential. However, the exact mechanism by which platelet levels are rapidly regenerated after acute inflammation remains unknown.

Here, we report the existence of potent stem-like Mk-committed progenitors (SL-MkPs) within the phenotypic HSC compartment. Under stress conditions like viral infections, acute inflammatory signaling triggers cell cycle activation of quiescent SL-MkPs and Mk protein production, which drives a rapid maturation program of SL-MkPs and other MkPs. Together, this mediates an efficient platelet recovery after inflammation-induced thrombocytopenia.

RESULTS

Inflammatory Signaling Drives Megakaryocytic Protein Expression in Phenotypic HSCs

Inflammatory signaling during infection triggers a rapid depletion of circulating platelets and other blood cells. To study the hematopoietic system during such stress conditions, we mimicked a viral infection by inducing acute inflammation through administration of a single dose of polyinosinic:polycytidylic acid (pI:C) to mice. As expected, inflammation was associated with dramatic reduction in platelet numbers, but homeostatic blood platelet levels were restored within a few days, suggesting intensive platelet regeneration (Figure 1A). To elucidate which cell types might be involved in this rapid platelet regeneration program, we measured the expression of CD41 (Itga2b), an early marker of megakaryocytic maturation, in distinct cell populations of the hematopoietic stem and progenitor cell compartment during homeostasis and 16 hr after pI:C induction (see Supplemental Information; Figures S1A–S1C for gating strategies under inflammation). In accordance with previous reports, CD41 was expressed in MkPs and at low levels in a subset of HSCs during homeostasis (Gekas and Graf, 2013). Unexpectedly, all investigated cell types potentially capable of generating Mks robustly increased CD41 protein expression upon pI:C treatment, including MkPs, MEPs, and, most surprisingly, phenotypic HSCs, whereas other cell types remained unaffected (Figure 1B). Since inflammation induced the strongest relative upregulation of CD41 in the HSC compartment, we subjected fluorescence activated cell sorting (FACS) purified HSCs ($Lin^-cKit^+CD150^+CD48^-$) and progenitors ($Lin^-cKit^+CD150^+CD48^+$) from control and pI:C treated mice to mass spectrometry-based quantitative proteomics in order to globally characterize inflammation-mediated changes in the HSC proteome. Of a total of 7,492 identified proteins, 162 proteins were significantly changed in HSCs upon induction of inflammation (Table S1). As expected, pI:C treatment triggered the production of typical interferon (IFN) response proteins (Figures 1C, 1D, S1D, and S1E), but also revealed a significant increase of 28 proteins typically expressed in mature Mks and platelets (Figures 1C, 1D, and S1E). These included CD41 (Itga2b) and its partner CD61 (Itgb3), components of the GPIb-IX-V complex, platelet-selectin (Selp), the platelet and Mk-specific β1 tubulin (Tubb1), as well as many proteins characteristic for Mk and platelet alpha-granules, such as Vwf and platelet factor 4 (Pf4). In concert with our finding that inflammation-driven Mk protein increase is highest in HSCs (Figure 1B), the upregulation of Mk proteins in $Lin^-cKit^+CD150^+CD48^+$ progenitors was almost absent (Figures 1C, 1D, S1E, and S1F).

Since pI:C administration triggers a wide production and secretion of type-I IFNs in vivo, we hypothesized that type-I IFN signaling might be involved in regulating the production of Mk proteins in HSCs. Accordingly, administration of recombinant IFNα phenocopied pI:C injections with regards to Mk protein upregulation (Figure S1G), and the pI:C-mediated increase in Mk proteins was completely absent in HSCs from IFNα receptor (IFNAR) knockout mice (Figures 1D and S1E). The analysis of forward, reverse, and 50:50 wild-type (WT):$IFNAR^{-/-}$ bone marrow chimeras revealed that type-I IFN signaling directly instructs Mk protein expression in phenotypic HSCs (Figure S1H). Canonical type-I IFN signaling results in the activation of the signal transducer STAT1 and crosstalk signaling to mTOR has been reported (Platanias, 2005). Therefore, we investigated the involvement of STAT1 and mTOR in pI:C-mediated Mk protein upregulation. Either the pharmacological inhibition of mTOR using rapamycin or the genetic deletion of STAT1 reduced inflammation-mediated Mk protein upregulation, suggesting that both pathways participate in the regulation of Mk protein production in HSCs (Figures S1I–S1K). In contrast, stem cell antigen 1 (Sca-1), involved in pI:C-induced cell cycle activation of HSCs, was not required for pI:C-induced Mk protein expression (Figure S1L). Moreover, single administrations of lipopolysaccharide (LPS), mimicking a bacterial infection, or recombinant tumor necrosis factor alpha (TNFα), a cytokine involved in mediating acute inflammation, also triggered an increase of Mk proteins in HSCs comparable to pI:C (Figure 1E). In contrast to pI:C, LPS-mediated Mk protein expression in HSCs was mediated by TLR4/MYD88/TRIF-signaling (Figure S1M). Reducing platelet levels using a platelet depletion antibody without triggering inflammation induced only a minor increase of Mk proteins, further highlighting the importance of inflammatory signaling (Figure S1N). Together, these data demonstrate that inflammatory signaling associated with infections directly triggers Mk protein expression in phenotypic HSCs.

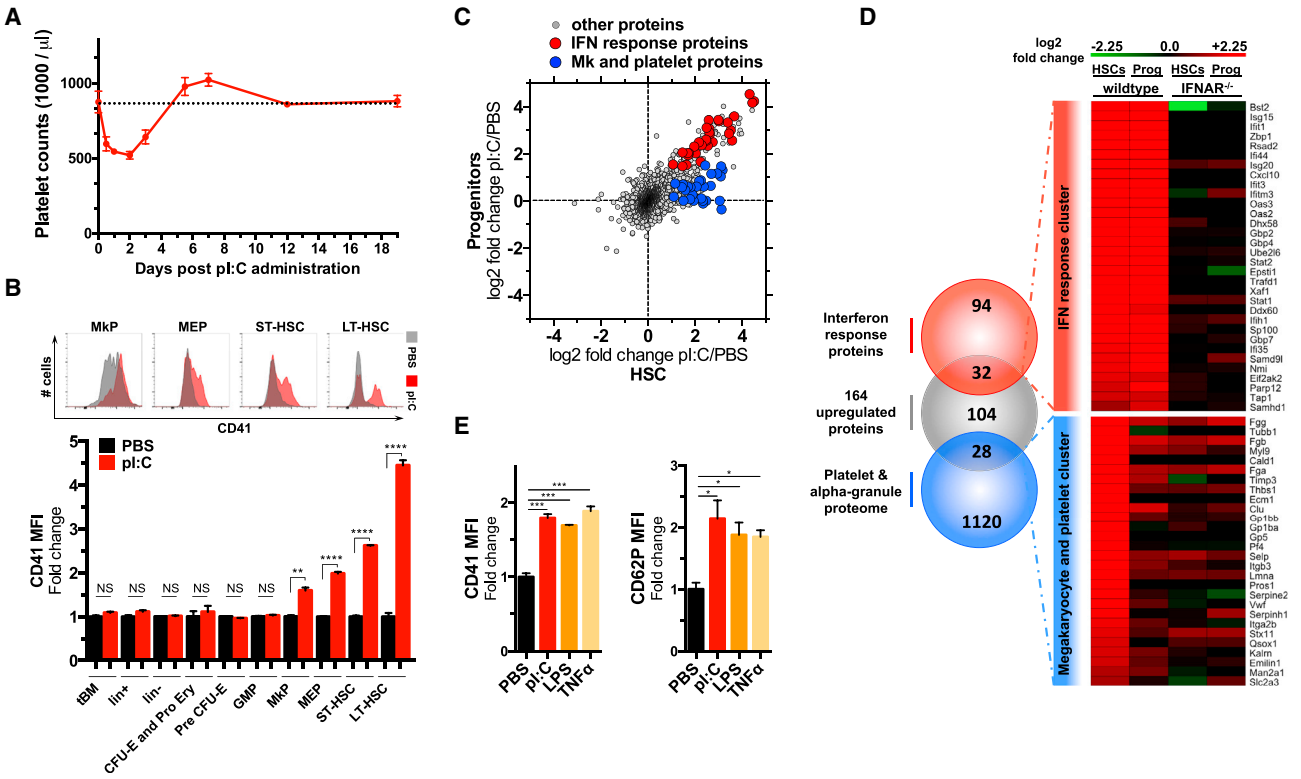

Figure 1. Inflammation Drives Megakaryocytic Protein Expression in HSCs

(A) Platelet counts upon treatment with pI:C.

(B) Flow cytometric analysis of CD41 expression in distinct stem and progenitor compartments of PBS and pI:C treated mice 16 hr after injection.

(C and D) Mass spectrometry-based quantitative proteome analysis of HSCs ($Lin^-cKit^+CD150^+CD48^-$) and progenitors ($Lin^-cKit^+CD150^+CD48^+$) isolated from WT and $IFNAR^{-/-}$ mice 16 hr after PBS or pI:C treatment.

(C) Scatter plot of fold changes in protein levels upon pI:C treatment in HSCs and progenitors of WT mice.

(D) Heatmap illustrating protein log2 fold changes upon pI:C treatment in WT and $IFNAR^{-/-}$ HSCs and progenitors for the overlapping proteins of the Venn diagram.

(E) Flow cytometric analysis of CD41 and CD62P expression in HSCs 16 hr after pI:C, LPS and TNFα administration.

In (A), (B), and (E), data are presented as mean ± SEM with $n \geq 3$. The significance was determined using an unpaired, two-tailed student's t test (*$p \leq 0.05$, **$p \leq 0.01$, ***$p \leq 0.001$, ****$p \leq 0.0001$, and non-significant: NS). See also Figure S1.

SL-MkPs within the Phenotypic HSC Compartment Increase Mk Protein Expression upon Acute Inflammation

Recent reports identified multipotent HSCs with intrisinc Mk bias as well as unipotent Mk-committed progenitors in the phenotypic HSC compartment (Sanjuan-Pla et al., 2013; Shin et al., 2014; Yamamoto et al., 2013). To determine whether inflammation-driven Mk protein expression takes place primarily in multipotent HSCs or in other cell types present in the phenotypic HSCs compartment and to investigate whether elevated Mk protein levels are associated with Mk lineage fate decisions, we made use of high-throughput single-cell ex vivo lineage tracking (Figure 2A). Single LT-HSCs were sorted into differentiation medium containing fluorescently labeled antibodies, and the morphology and expression of lineage makers of individual cells was tracked in clonally expanded progeny by daily fluorescence microscopy. This allowed a time-resolved analysis of ex vivo differentiation in a quantitative manner. As expected, the majority of HSCs from homeostatic mice formed large "*mixed*" colonies containing both myeloid and megakaryocytic cells. However, a fraction of the phenotypic HSCs generated exclusively mature Mks, suggesting that these cells were committed to Mk-lineage (Figures 2B, S2A, and S2B). This sets them apart from multipotent, but Mk-biased, populations such as *Vwf*$^+$ HSCs (Sanjuan-Pla et al., 2013), but is in accordance with a recent single-cell transplantation study identifying Mk-committed progenitors with high self-renewal potential in the HSC compartment (Yamamoto et al., 2013). While some phenotypic HSCs directly gave rise to single Mks, others formed large colonies consisting of up to hundreds of mature Mks (Figures S2A and S2B). These potent stem cell-like megakaryocyte-committed progenitors (SL-MkPs) are distinct to classical MkPs and exist within the phenotypic HSC pool during homeostasis (Figures S2A and S2B). The number of single-sorted HSCs giving rise to "*Mk only*" colonies during homeostasis and inflammation was the same (Figure 2B), suggesting that commitment of multipotent HSCs to SL-MkPs occurs during homeostasis, and inflammatory signaling induces Mk protein expression without affecting lineage fate decisions. To determine which cell types increase Mk protein levels upon inflammation, we retrospectively assigned CD41 fluorescence intensity values

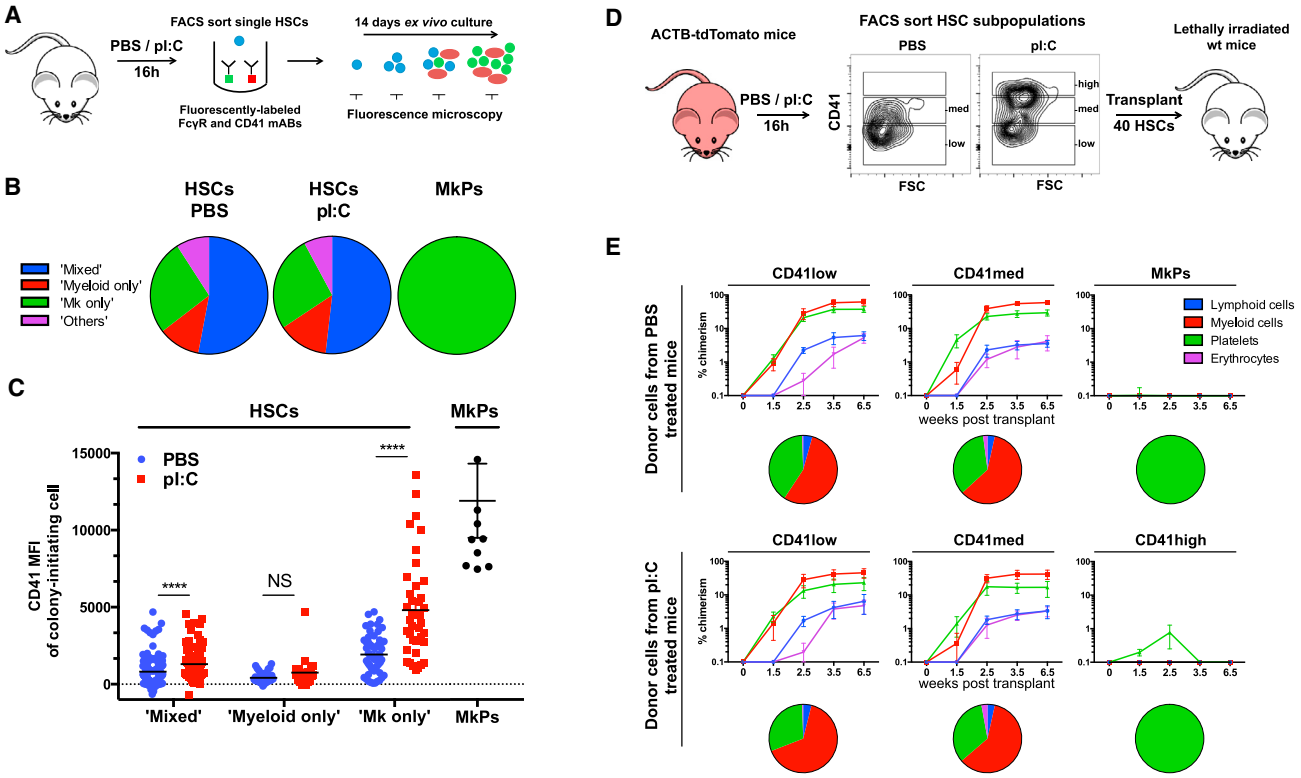

Figure 2. Stem-like Mk-Committed Progenitors within the Phenotypic HSC Compartment Increase Mk Protein Levels upon Acute Inflammation

(A–C) Ex vivo lineage tracking of single LT-HSCs from PBS and pI:C treated mice. The representative data for one out of two independently performed experiments is shown. (A) Illustration of experimental approach. (B) Distribution of colony types formed at day 14 of ex vivo liquid culture. (C) CD41 surface expression of single-sorted LT-HSCs and MkPs giving rise to the indicated colony types.

(D and E) Transplantation of LT-HSC CD41 sub-populations. The ACTB-Tomato mice were treated with PBS or pI:C, after 16 hr, 40 LT-HSCs or 300 MkPs were transplanted into lethally irradiated WT recipients. (D) Illustration of experimental approach. (E) Results. The pie charts represent relative lineage contributions. For (C) and (E), the data are presented as mean ± SEM. The significance was determined using a Mann-Whitney-Wilcoxon test (*p ≤ 0.05, **p ≤ 0.01, ***p ≤ 0.001, ****p ≤ 0.0001, and non-significant: NS). See also Figure S2.

from single-sorted HSCs to the colony types they formed (Figure 2C). Phenotypic HSCs generating mixed colonies showed minor, but significant, increase in CD41 expression upon inflammation, whereas cells generating "*myeloid only*" colonies remained unaffected from CD41 upregulation. In contrast, SL-MkPs (i.e., cells giving rise to Mk only colonies) robustly increased CD41 expression to elevated levels upon inflammation, suggesting that SL-MkPs are the primary source of Mk protein expression upon pI:C treatment within the phenotypic HSC compartment.

To confirm this finding in vivo, we sub-fractionated LT-HSCs from ACTB-tdTomato mice based on their CD41 signal into CD41*low* and *med* for PBS treated mice and CD41*low*, *med*, and *high* for pI:C treated mice and traced the generation of tomato-positive lineage cells in the blood (Figures 2D and 2E). In line with our single-cell ex vivo data, CD41*low* and CD41*med* HSCs from both PBS and pI:C treated mice showed multilineage reconstitution (Gekas and Graf, 2013), whereas CD41*high* HSCs from pI:C treated mice exclusively generated platelets in a transient manner, demonstrating that these cells were committed to the Mk lineage (Figure 2E). In contrast, MkPs generated a much lower platelet chimerism, confirming that CD41*high* HSCs represent potent SL-MkPs that are superior to classical MkPs in their platelet generation capacity. Together, these data demonstrate that commitment of HSCs to SL-MkPs appears during homeostasis. While SL-MkPs express similar levels of Mk proteins compared to HSCs during homeostasis, inflammatory signaling triggers Mk protein expression in SL-MkPs without affecting lineage commitment of HSCs to SL-MkPs.

Inflammation Drives Functional and Cellular Maturation of SL-MkPs and MkPs

To investigate whether increased Mk protein expression might be attributed to an inflammation-driven maturation of SL-MkPs, we performed kinetic analyses of Mk generation ex vivo. While single-sorted control MkPs did not expand, form small Mk colonies, and mature within the first 2–3 days in culture, SL-MkPs (phenotypic HSCs generating Mk only colonies) from homeostatic mice expanded in an immature state until day 7–8, matured late, and formed large Mk colonies (Figures 3A, S2B, and S2C). In contrast, SL-MkPs from pI:C treated mice generated mature Mks much faster (Figures 3A and S2C), suggesting that inflammation triggered efficient maturation of SL-MkPs. The induced maturation of SL-MkPs was associated with a reduced expansion of immature cells and thus with a

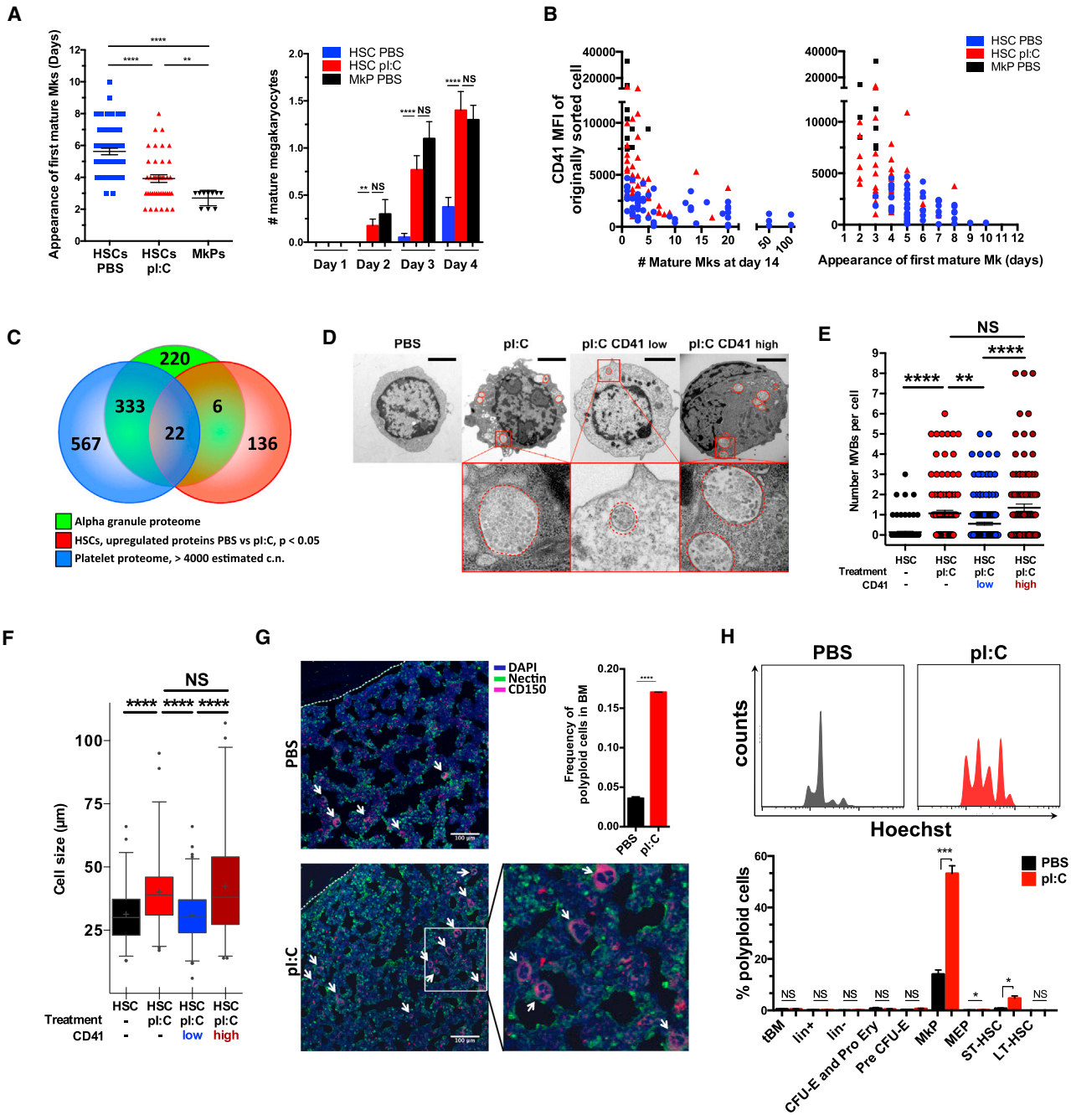

Figure 3. Inflammation Drives a Cellular Mk Maturation Program at Distinct Levels of Megakaryopoiesis

(A) Time until first mature Mk cell appears in the culture of Mk only colonies (left). The mean number of mature Mks at day 1–4 after culture of Mk only colonies (right).

(B) Mk colony size (left) and Mk maturation time (right) of Mk only colonies anti-correlate with CD41 protein expression of originally sorted LT-HSCs (i.e., SL-MkPs). The Mk colony size was determined on day 14 of culture.

(C) Venn diagram illustrating that Mk proteins upregulated in HSCs upon inflammation are typically localized to alpha-granules in platelets.

(D) Electron microscopy visualization of HSCs, CD41low, and CD41high HSCs from PBS and pI:C treated mice 16 hr after treatment. The MVBs are marked in red.

(E) Quantification of MVBs.

(F) Quantification of cell size based on stereology analysis of electron micrographs.

(G) Bone sections and quantification of polyploid Mks. The bone sections were stained with CD150 (red), Nectin (green), and DAPI (blue) 16 hr after treatment. The polyploid Mks were quantified using Hoechst staining and FACS.

(H) Quantification of polyploidy in stem and progenitor cell populations 16 hr after PBS and pI:C treatment. The representative histogram of MkPs is shown at the top. In (A), (E), (G), and (H), data are presented as mean ± SEM with n ≥ 3. The significance was determined using a Mann-Whitney-Wilcoxon test (A and E), or an unpaired, two-tailed student's t test (G and H) (*p ≤ 0.05, **p ≤ 0.01, ***p ≤ 0.001, ****p ≤ 0.0001, and non-significant: NS). See also Figure S3.

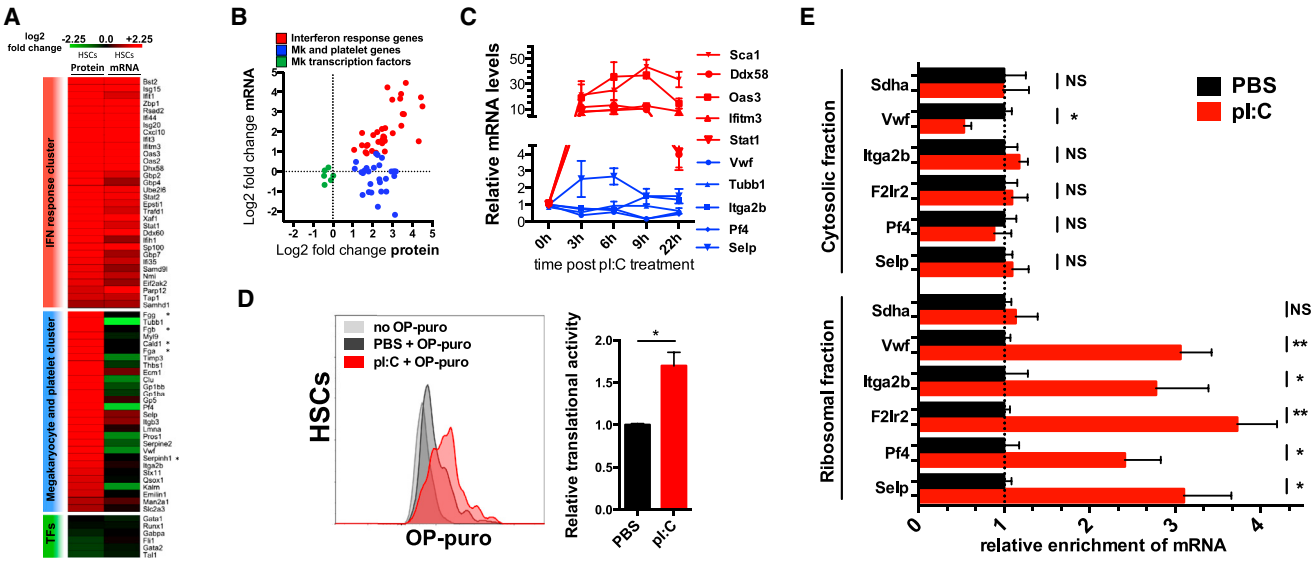

Figure 4. Megakaryocytic Protein Upregulation in HSCs Is Mediated by a Post-Transcriptional Mechanism

(A) Comparison of log2 fold changes in protein level and transcript level of HSCs, isolated from PBS and pI:C treated mice, 16 hr after treatment. The protein and transcript levels derived from proteomics and qPCR, respectively. The genes marked with asterisks were not detected on transcript level.

(B) Scatterplot view from data presented in (A).

(C) Time-course qPCR analysis of Mk (blue) and IFN response gene (red) transcripts at indicated time points after treatment with pI:C in HSCs.

(D) Translational activity of HSCs upon inflammation. The OP-Puro incorporation was measured 16 hr after PBS/pI:C and 1.5 hr after OP-Puro administration (see Supplemental Information).

(E) Ribosomal profiling of Mk transcripts upon inflammation. The mRNA levels of housekeeping (Sdha) and Mk genes (others) were measured in both fractions and normalized to Actb.

In (C)–(E), data are presented as mean ± SEM with $n \geq 3$. The significance was determined using an unpaired, two-tailed student's t test (*$p \leq 0.05$, **$p \leq 0.01$, ***$p \leq 0.001$, ****$p \leq 0.0001$, and non-significant: NS). See also Figure S4.

smaller overall size of Mk colonies (Figure S2C). Interestingly, CD41 expression of the colony-initiating SL-MkPs and MkPs was anti-correlative with both the expansion potency of the cell and with the time required to generate the first mature Mk (Figure 3B). Hence, the most primitive SL-MkPs with low Mk protein expression generate the largest Mk colonies at late time points, while cells with high Mk protein expression generate smaller Mk colonies at early time points. In contrast to SL-MkPs, inflammation had no impact on Mk maturation time or the overall amount of mature Mks generated from HSCs with mixed colony potential (Figure S2C).

Alpha granules or their precursors in the form of multivesicular bodies (MVBs) are typical features of megakaryocytic maturation (Heijnen et al., 1998). Comparison of Mk proteins that were synthesized upon inflammation in HSCs with the platelet alpha-granule proteome (Browne et al., 2001) revealed that the majority of these proteins are typically localized to alpha granules (Figure 3C). In accordance with this, electron microscopy and immunofluorescence microscopy of purified HSCs revealed the generation of MVB-like structures 16 hr after induction of inflammation, which was correlated with the upregulation of Mk proteins and was a particularly frequent event in CD41^{high} SL-MkPs (Figures 3D, 3E, and S3A–S3C). Electron microscopy and FACS analysis revealed an IFNAR-STAT1 and mTOR dependent cell size increase of HSCs, which was particularly attributed to SL-MkPs that upregulate Mk proteins (Figures 3F, S3D, and S3E).

Polyploidy is a characteristic feature of terminally maturated Mks (Machlus and Italiano, 2013). A strong increase in the number of polyploid Mks was observed 16 hr after pI:C treatment (Figure 3G). Quantifying ploidy levels in stem and progenitor cell populations revealed that, in particular, MkPs were driven into endomitosis in an IFNAR-STAT1 dependent manner, whereas phenotypic LT-HSCs did not enter endomitosis (Figures 3H and S3F). Together, these data suggest that inflammation drives a rapid and efficient cellular maturation program of both SL-MkPs and MkPs. SL-MkPs are maintained in a highly potent and primitive state during homeostasis, but are efficiently pushed toward maturation upon inflammation, adapting an intermediate state between homeostatic SL-MkPs and classical MkPs. In contrast to classical MkPs, which are driven into endomitosis forming mature Mks, SL-MkPs are pushed toward maturation without directly undergoing endomitosis, thereby maintaining their high proliferative expansion capacity.

Inflammation-Driven Upregulation of Megakaryocytic Proteins in Phenotypic HSCs Is Mediated by a Post-Transcriptional Mechanism

To determine whether the increase in Mk proteins is transcriptionally controlled, we compared transcript and protein levels of HSCs 16 hr after induction of inflammation. As expected, IFN response genes were regulated at the transcriptional level with a high induction of transcripts, resulting in enhanced protein production (Figures 4A, 4B, and S4A) (Platanias, 2005). In contrast, Mk genes remained unchanged or were even downregulated at the transcriptional level, while the corresponding proteins were significantly increased (Figures 4A, 4B,

and S4A), suggesting a pI:C-induced non-transcriptional regulation of Mk protein expression. In accordance with this, transcription factors regulating Mk gene transcription remained unaffected at the transcript and protein level (Figures 4A, 4B, and S4A). Time course experiments demonstrated a rapid transcriptional induction of IFN response genes, whereas Mk transcripts showed no or only minor increase, excluding the possibility of elevated protein levels caused by an early transcriptional induction of Mk genes (Figure 4C). Several scenarios are conceivable to explain such a non-transcriptional increase in Mk proteins. Whole platelets, or platelet-derived microparticles (PMPs) containing Mk proteins, may adhere to or be taken up by HSCs. However, antibody-mediated depletion of platelets did not affect pI:C-mediated Mk protein increase, suggesting that Mk proteins were not of platelet origin (Figure S4B). Since most Mk transcripts were detected at high levels in HSCs, we reasoned that inflammation-mediated Mk protein production might be a result of increased translation of transcripts that are already present during homeostasis. To measure global levels of translation in phenotypic HSCs, we made use of an O-propargyl-puromycin (OP-Puro)-based method, which facilitates the measurement of translational rates on single-cell level in vivo (Liu et al., 2012; Signer et al., 2014). In accordance with a recent study, homeostatic HSCs showed very low levels of translational activity (Signer et al., 2014), but had significantly increased translational rates upon pI:C treatment (Figure 4D). Importantly, increased translational activity correlated with enhanced Mk protein expression (Figure S4C). In accordance with an enhanced translational activity, phenotypic HSCs demonstrated reduced levels of the translation inhibitors Pdcd4 and Eef2k upon pI:C treatment, which negatively regulate the translation initiation and elongation factors Eif4a and Eef2 (Dorrello et al., 2006; Kruiswijk et al., 2012) (Figure S4D). Occupancy of transcripts at ribosomes is a strong indication of translational activity (Ingolia et al., 2012). Accordingly, Mk transcript occupancy at ribosomes significantly increased upon induction of inflammation, suggesting enhanced translation of these transcripts (Figures 4E and S4E). Together, these experiments suggest that even though most Mk transcripts are expressed in phenotypic HSCs, translation of these transcripts is repressed during homeostasis. In contrast, pI:C treatment instructs efficient translation, resulting in an enhanced Mk protein production.

SL-MkP Commitment Is Associated with a Coordinated Mk Transcription Program Providing Transcriptional Templates for Inflammation-Driven Protein Synthesis

Even though high expression of Mk transcripts in phenotypic HSCs has been well documented (Gekas and Graf, 2013; Månsson et al., 2007; Sanjuan-Pla et al., 2013), the mechanistic role of transcriptional priming is poorly understood. Our data suggest that Mk transcripts are expressed during homeostasis and serve as a template for an efficient inflammation-induced emergency Mk protein synthesis program in SL-MkPs. According to this model, high expression of Mk transcripts in SL-MkPs would be required for mounting an efficient inflammation-mediated post-transcriptional increase in Mk proteins, whereas low Mk transcriptional priming in HSCs would explain their attenuated response.

To characterize Mk lineage priming in HSCs, SL-MkPs, and classical MkPs, we measured Mk and control transcripts of individual MkPs and CD41 sub-populations of LT-HSCs from PBS and pI:C treated mice by single-cell quantitative (q)PCR. In accordance with a previous report, all investigated Mk transcripts were expressed in a bimodal fashion in HSCs, with Cycle-threshold differences (ΔCt) of 15-20 between high-expressing cells and low-expressing cells, suggesting that Mk transcripts are expressed in an "ON" or "OFF" state (Figure 5A) (Guo et al., 2013). Heatmap representation and principal component analysis (PCA) of this data revealed that all MkPs expressed Mk transcripts to high homogenous levels, whereas most LT-HSCs with homeostatic CD41 levels (CD41*low/med* HSCs) expressed a unique combination of Mk transcripts in the ON or OFF state. This was reflected in a funnel-shaped cloud, with each cell occupying a unique location in our PCA analysis, suggesting a stochastic Mk transcript expression (Figures 5B and 5C). Interestingly, some homeostatic LT-HSCs clustered together at the tip of the funnel, representing cells with a coordinated Mk transcription profile with all Mk transcripts in the ON state. Of note, almost all CD41*high* HSCs from pI:C treated mice (i.e., SL-MkPs) expressed all Mk transcripts in the ON state and clustered together with these cells at the tip of the funnel (Figures 5B–5D), demonstrating that homeostatic SL-MkPs exhibit a coordinated Mk transcription profile and efficiently upregulate Mk protein synthesis upon inflammation. The hypothesis that commitment of HSCs to SL-MkPs is associated with a switch from a stochastic toward a coordinated Mk transcription program was further supported by a significant drop in the Fano factor, an indicator for a system's stochasticity and transcriptional noise (Figure S5A) (Munsky et al., 2012; Ozbudak et al., 2002).

Profiling of transcription factors (TFs) in single HSCs revealed that expression of many known Mk TFs correlated with Mk-commitment (e.g., highest expression in classical MkPs and SL-MkPs) and expression of Mk lineage transcripts (Figures S5B–S5D). This suggests that Mk transcriptional priming and Mk lineage commitment of SL-MkPs are established by transcriptional regulators during homeostasis, while inflammation drives a post-transcriptional Mk protein synthesis from these pre-existing transcripts.

To investigate how closely related multipotent HSCs and SL-MkPs are, we performed global gene expression analysis of single HSCs and $Lin^{-}cKit^{+}CD150^{-}$ progenitors using a customized single-cell RNA-sequencing (seq) approach. In accordance with our single-cell qPCR data, Mk transcripts were significantly enriched among the most variably expressed genes and Mk lineage priming differed dramatically between individual HSCs, whereas progenitors consistently showed little or no Mk lineage transcript expression (Figures S5E, 5E, and 5F). To determine whether the transcriptome of HSCs with high Mk lineage priming differs from HSCs with low Mk lineage priming, we performed PCA of HSCs and color-coded each cell with a calculated Mk Gene Set Enrichment Analysis (GSEA)-score reflecting the degree of Mk lineage priming (Figure 5G). Importantly, genome-wide expression profiles did not correlate with the degree of Mk-lineage priming, suggesting that Mk-primed HSCs (e.g., SL-MkPs) and HSCs with low Mk lineage priming are highly related cell types. Together, these data suggest that multipotent

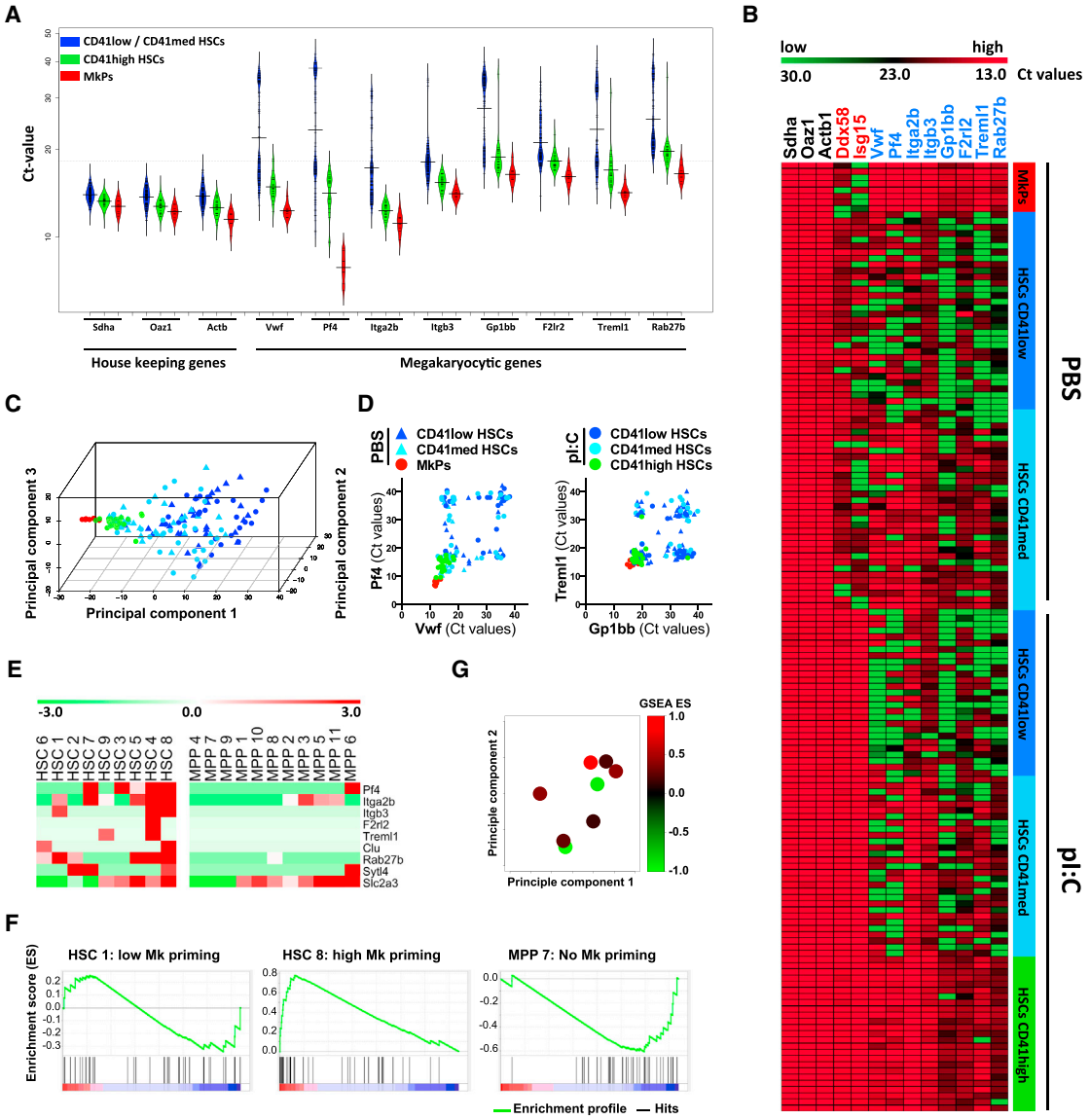

Figure 5. HSCs Switch from a Stochastic to a Coordinated Mk Transcript Expression Program upon Commitment from Multipotency toward the Mk Lineage

(A–D) Single-cell qPCR of LT-HSC CD41 sub-populations. (A) Bean plot representation of Mk transcripts of MkPs and LT-HSCs with homeostatic CD41 expression (CD41low and CD41med) of PBS or pI:C treated mice or with elevated CD41 levels (CD41high and SL-MkPs) of pI:C treated mice. (B) Heatmap indicating transcript expression of housekeeping genes (Sdha, Oaz1, and Actb), IFN response genes (Ddx58 and Isg15), and Mk genes (others). (C) PCA of CD41 sub-populations of LT-HSCs based on their Mk transcript expression values. The labels are as indicated in (D). (D) Transcript expression of Vwf versus Pf4 (left) and Treml1 versus Gp1bb (right). The expression values are presented as Ct-values.

(E–G) Single-cell RNA-seq of Lin$^-$cKit$^+$CD150$^+$CD48$^-$ HSCs and Lin$^-$cKit$^+$C150$^-$ progenitors. (E) Heatmap of HSCs and progenitors showing expression of Mk and platelet cluster genes in individual cells that were detected with at least 50 reads per cell on average and were significantly differentially expressed. (F) GSEA of Mk cluster genes in single HSCs and progenitors. The exemplary GSEA profiles are shown. (G) PCA of HSCs based on their overall transcriptome. The individual cells are color-coded according to their Mk GSEA enrichment score (ES). See also Figure S5.

HSCs and SL-MkPs exhibit a related overall transcriptome, however, commitment from multipotent HSCs to SL-MkPs is associated with a switch from a stochastic to a coordinated Mk transcription program. High transcriptional Mk priming provides SL-MkPs with the appropriate transcripts to mount an efficient post-transcriptional Mk protein synthesis program upon inflammatory signaling.

SL-MkPs Represent an Mk-Committed Sub-Population of VWF$^+$ HSCs

VWF$^+$ HSCs represent a multipotent, but Mk-biased, sub-population of HSCs that has been defined by high transcriptional expression of the *Vwf* gene (Sanjuan-Pla et al., 2013). To directly compare SL-MkPs with VWF$^+$ HSCs, we separated LT-HSCs depending on their *Vwf* transcriptional activity (Figure S5F).

VWF$^+$ HSCs showed an enriched Mk transcriptional priming if compared to VWF$^-$ HSCs (Figure S5F) (Sanjuan-Pla et al., 2013). However, only a small sub-fraction of VWF$^+$ HSCs showed expression of all Mk transcripts. In contrast, SL-MkPs uniformly showed high expression of all Mk genes including *Vwf,* correlating with their commitment to the Mk-lineage. Thus, SL-MkPs represent an Mk-committed sub-population of VWF$^+$ HSCs. These data are consistent with a model where VWF$^+$ HSCs preferentially give rise to SL-MkPs, thereby establishing the Mk-bias of multipotent VWF$^+$ HSCs.

The Most Potent and Primitive SL-MkPs Reside in a Dormant State and Are Efficiently Activated upon Inflammation

The most potent HSCs are maintained in a long-term quiescent (dormant) state where they serve as a reserve pool for conditions of acute stress (Wilson et al., 2008). Long-term quiescent, label-retaining cells (LRCs) can be identified in the HSC compartment using doxycyclin (dox) treatment of SCL-tTA:H2B-GFP mice (Wilson et al., 2008). Whether dormant lineage-restricted progenitors exist in the phenotypic HSC compartment is unknown. Interestingly, an inflammation-mediated increase in Mk protein expression, cell size, and granularity could be observed both in non-LRC LT-HSCs and in dormant LRC LT-HSCs, suggesting that SL-MkPs also exist in a dormant state (Figures 6A–6C, S6A, and S6B). Accordingly, single-cell ex vivo lineage tracking showed that SL-MkPs exclusively generating mature Mks could be found both in the non-LRC fraction and in the dormant LRC fraction of the LT-HSC compartment. Interestingly, dormant SL-MkPs formed larger Mk-colonies and required a longer time to generate the first mature Mks when compared to their non-LRC counterparts (Figure 6D). This suggests that the most primitive and most potent SL-MkPs reside in a dormant state and, hence, do not contribute to steady-state megakaryopoiesis.

To investigate whether quiescent SL-MkPs are activated upon inflammation, we measured cell cycle activity in HSC CD41 sub-populations. Ki67-Hoechst and BrdU incorporation assays revealed a rapid and efficient cell cycle entry of SL-MkPs that increased Mk protein levels 16 hr post pI:C treatment, whereas the remaining HSC pool was activated at later time points (Figures 6E–6G and S6E). Accordingly, inflammation triggered by LPS or TNFα injection resulted in a similar cell cycle induction of these SL-MkPs that increased Mk protein levels (Figure S6C), demonstrating that distinct inflammatory signals efficiently activate quiescent SL-MkPs.

FoxO3a is a key TF that instructs transcription of the cell cycle inhibitors p27, p57, p107, and p130, thereby maintaining HSCs in a quiescent state (Miyamoto et al., 2007; Tothova and Gilliland, 2007). Cell cycle entry of HSCs is frequently associated with FoxO3a phosphorylation and subsequent exclusion from the nucleus (Tothova and Gilliland, 2007). In phenotypic HSCs from control mice and HSCs from pI:C treated mice with homeostatic CD41 expression, FoxO3a was localized mainly to the nucleus. In contrast, in CD41*high* HSCs (i.e., SL-MkPs) from pI:C treated mice, FoxO3a was frequently redirected to the cytoplasm, suggesting that FoxO3a inactivation is associated with inflammation-induced cell cycle entry of SL-MkPs (Figures 6H and S6D). In accordance, a significant decrease in expression of FoxO3a targets p27, p57, p107, and p130 was specifically observed in SL-MkPs that increased Mk proteins, whereas p19, which is not a FoxO3a target, remained unchanged (Figure 6I). Together, these data suggest that acute inflammation triggers FoxO3a inactivation and efficient cell cycle activation of quiescent SL-MkPs.

Repeated Cycles of Type-I IFN Mediated Inflammation Trigger the Exhaustion of SL-MkPs and Other Megakaryocytic Progenitors

We have shown that a single induction of inflammation drives maturation of SL-MkPs and MkPs. Accordingly, repeated cycles of inflammation over a long time period would be anticipated to result in an exhaustion of these cell types. To investigate this hypothesis, mice were treated with pI:C every 3 days for a time period of 30 days (ten doses) (Figure 7A). While a single pI:C dose resulted in an augmented Mk protein production in HSCs and MkPs, as well as in an increase in mature polyploid Mks as described above, inflammation-mediated Mk protein production and the number of MkPs and mature polyploid Mks was significantly reduced upon repeated doses of pI:C (Figures 7B–7D). Regeneration from platelet consumption after single pI:C treatment was accomplished within 7 days, whereas after ten doses, the hematopoietic system required longer to rebuild the platelet pool, reflecting the reduction in MkPs and SL-MkPs (Figure 7E). These data indicate that repeated cycles of pI:C-mediated inflammation can result in a transient exhaustion of MkPs and SL-MkPs due to a constant drive toward maturation, which prevents an efficient platelet recovery after inflammation-mediated platelet loss.

DISCUSSION

During infection, platelets actively counteract infectious agents by releasing immunomodulatory agents and interacting with neutrophils to trap pathogens (Jenne et al., 2013; Yeaman, 2014), thereby, being rapidly consumed. Since low platelet levels during inflammation are associated with loss of vascular integrity and septic shock (Goerge et al., 2008; Xiang et al., 2013), a rapid recovery of platelet levels is of fundamental importance. We show that inflammatory signaling instructs a rapid Mk maturation program at distinct levels of megakaryopoiesis to regenerate the lost platelet pool. While MkPs are efficiently driven into endomitosis, leading to a strong increase in mature Mks, a small pool of potent Mk-committed progenitors (SL-MkPs) within the phenotypic HSC compartment replaces the lost MkPs. Even though SL-MkPs and classical MkPs appear to be closely related in their lineage potential and their coordinated Mk transcription profile, SL-MkPs share many features with HSCs which set them apart from MkPs. Similar to HSCs, and in contrast to MkPs, SL-MkPs are small in cell size, suppress Mk protein production, and are mainly quiescent. Due to their quiescent, partly dormant nature, SL-MkPs contribute little to steady-state megakaryopoiesis, but serve as an emergency pool for inflammatory insult.

As a result of their quiescence and the suppression of Mk protein production, SL-MkPs are maintained in a metabolically inactive, but primed, state, allowing them to be readily activated. Inflammatory signaling triggers FoxO3a inactivation, resulting in cell cycle activation of quiescent SL-MkP. Moreover, inflammation-mediated maturation of SL-MkPs is associated with mTOR

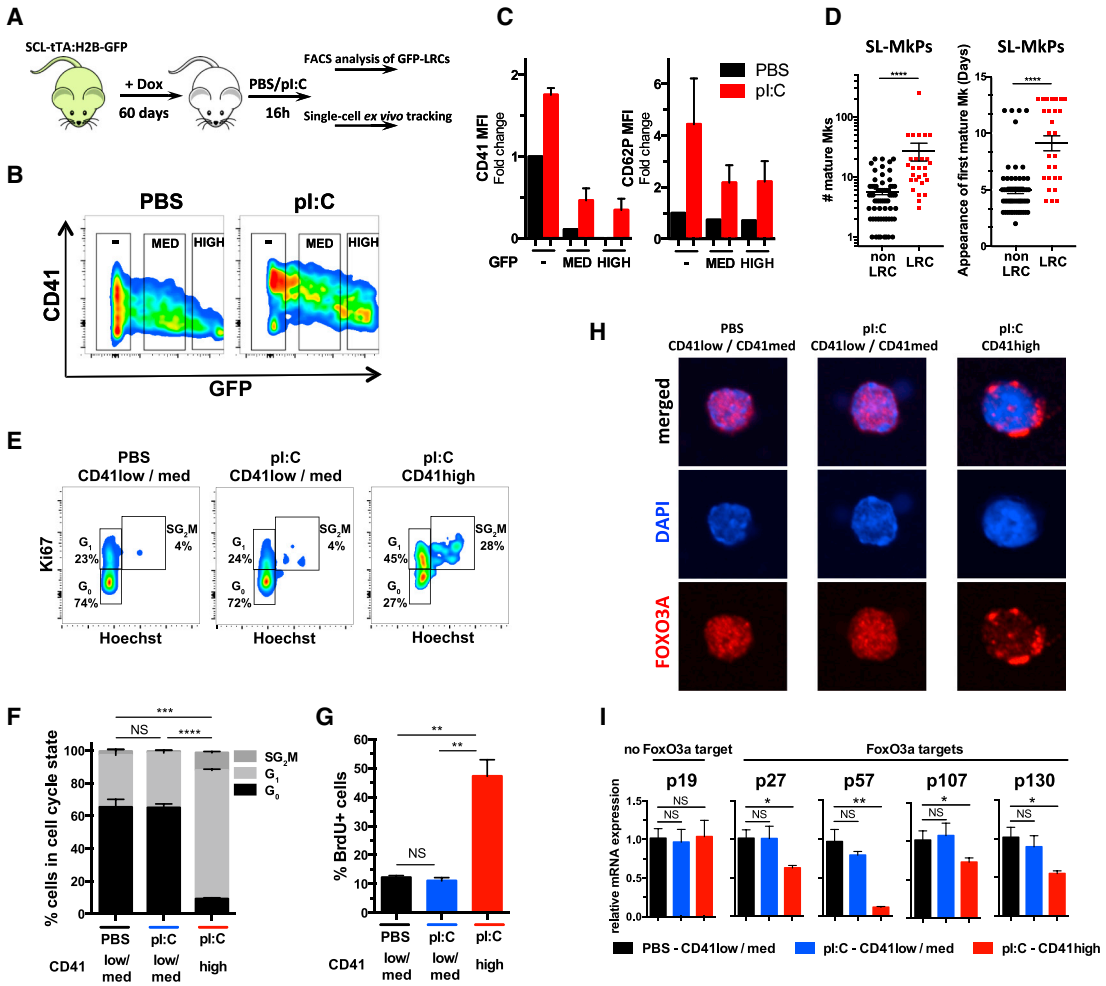

Figure 6. The Most Potent and Primitive SL-MkPs Reside in a Dormant State and Are Efficiently Activated upon Inflammation

(A–D) LRC assays. The dormant HSCs were labeled by administering dox to SCL-tTA:H2B-GFP mice for 60 days, followed by PBS or pI:C treatment. Subsequently, Mk protein expression was measured in HSCs (B and C) or mice were subjected to single-cell ex vivo lineage tracking (D). (A) Illustration of experimental approach. (B) Representative FACS plots after 60 days of chase, followed by PBS or pI:C treatment, in LT-HSCs. (C) Quantification of Mk protein expression. (D) Mk only colonies formed from GFP^{low} non-LRC-HSCs and GFP^{high} LRC-HSCs. The number of mature Mks formed at day 14 of culture (left). The time until first mature Mk cell appears in the culture (right).

(E) Representative FACS plots of Ki67-Hoechst cell-cycle stainings of HSC CD41 sub-populations.

(F) Quantification of Ki67-Hoechst cell cycle measurements.

(G) Cell cycle analysis of HSC CD41 sub-populations measured by BrdU incorporation.

(H) Representative confocal microscopy images of indicated CD41 LT-HSCs sub-populations, stained for FoxO3a (red) and DAPI (blue).

(I) Transcript levels of cell cycle inhibitors measured by qPCR in CD41 sub-populations of LT-HSCs.

In (C), (D), (F), (G), and (I), data are presented as mean ± SEM with n ≥ 3. The significance was determined using the Mann-Whitney-Wilcoxon test (D) or an unpaired, two-tailed student's t test (F, G, and I) (*p ≤ 0.05, **p ≤ 0.01, ***p ≤ 0.001, ****p ≤ 0.0001, and non-significant: NS). See also Figure S6.

and STAT1 dependent increase in cell size, enhanced Mk protein production, and appearance of alpha granular precursors. In line with our findings, both mTOR and STAT1 signaling have been previously implicated in megakaryopoiesis (Huang et al., 2007; Raslova et al., 2006).

During homeostasis, post-transcriptional regulation of gene expression is a rare event in HSCs and changes in protein and mRNA levels are highly correlated during commitment (Cabezas-Wallscheid et al., 2014). In contrast to homeostasis, our findings reveal the presence of significant post-transcriptional regulation in response to acute inflammation. Our data suggest that Mk transcripts are expressed, but that translation is repressed during homeostasis, resulting in low Mk protein production, whereas inflammatory signaling drives efficient translation of these transcripts, revealing an important role for Mk lineage priming during emergency megakaryopoiesis. This model is supported by recent findings demonstrating that HSCs suppress protein synthesis during homeostasis (Signer et al., 2014). Our single-cell gene expression data provide novel insights into the basis of Mk lineage priming and suggest that multipotent HSCs and SL-MkPs exhibit highly related transcriptomes, but switch from a stochastic to a coordinated Mk

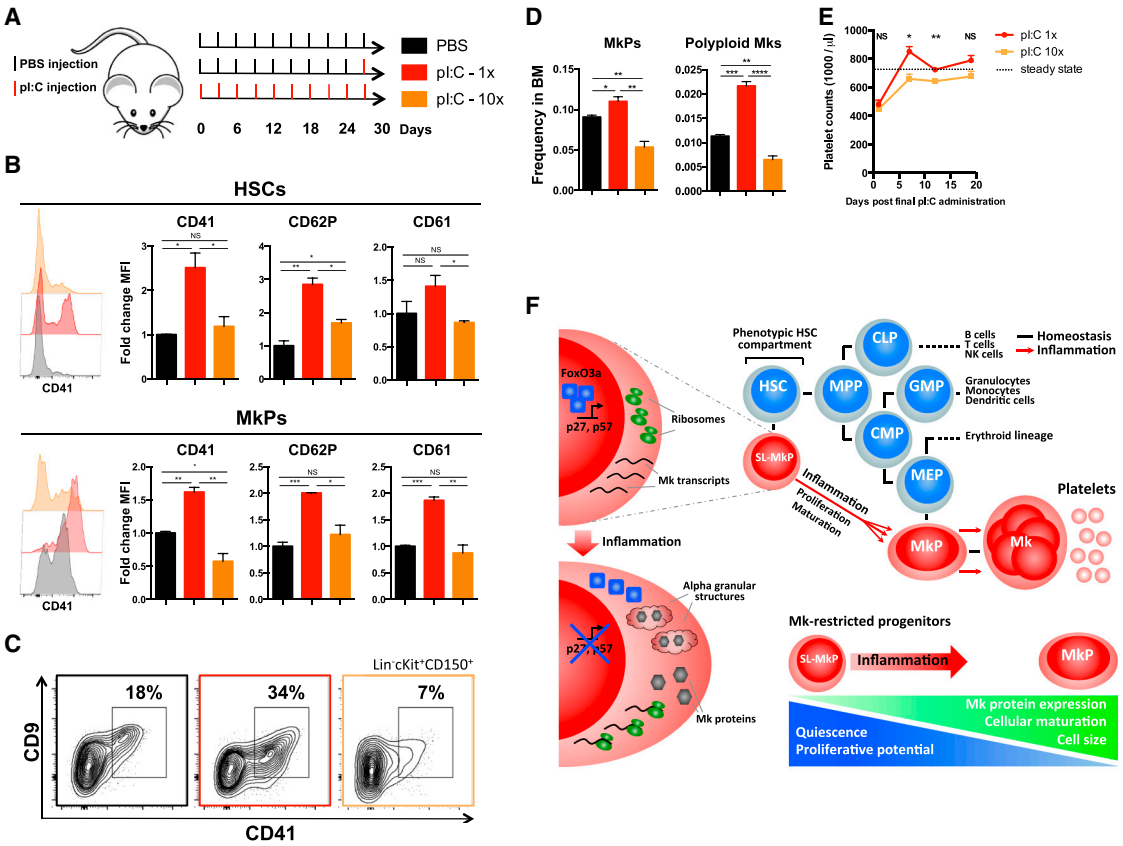

Figure 7. Chronic Inflammation Triggers Exhaustion of SL-MkPs and Other MkPs

(A–E) Mice were treated every third day for a 30 day period with pI:C. At 16 hr after the final administration, HSCs and MkPs were FACS-analyzed (B–D) or platelet recovery was investigated (E). For control purposes, mice were treated with PBS in the same schedule or with PBS and single final pI:C dose. (A) Illustration of experimental approach. (B) Flow cytometric analysis of Mk protein expression in HSCs or MkPs. (C) Representative FACS plot of Lin$^-$cKit$^+$CD150$^+$ bone marrow cells and CD41 and CD9 expression. (D) Quantification of MkPs and polyploid Mks. (E) Platelet recovery after chronic and acute inflammation.

(F) Model.

In (B), (D), and (E), data are presented as mean ± SEM with n ≥ 3. The significance was determined using an unpaired, two-tailed student's t test (*p ≤ 0.05, **p ≤ 0.01, ***p ≤ 0.001, ****p ≤ 0.0001, and non-significant: NS).

transcription program upon commitment from multipotent HSCs toward the Mk lineage.

Recent reports suggested the existence of Mk-biased, but multipotent, HSCs (Sanjuan-Pla et al., 2013; Shin et al., 2014). SL-MkPs represent a sub-population of VWF$^+$ HSCs, which in contrast to the VWF$^+$ HSCs are homogenously restricted to the Mk lineage reflected in their coordinated Mk transcription profile. A preferential commitment of Mk-biased HSCs to SL-MkPs could explain their intrinsic Mk lineage bias. In accordance with our data, single-cell transplantations of phenotypic HSCs revealed the existence of Mk-restricted progenitors with high self-renewal activity probably directly originating from HSCs (Yamamoto et al., 2013), likely representing the cells defined by our study as SL-MkPs.

In this study, we make use of CD41 expression to discriminate SL-MkPs during inflammation. During homeostasis, CD41 is expressed at low levels by HSCs and other myeloid progenitors (Gekas and Graf, 2013; Yamamoto et al., 2013). Due to an intrinsic repression of Mk protein synthesis, SL-MkPs express CD41 to similar levels as HSCs during homeostasis, but efficiently induce CD41 expression upon inflammatory signaling. This suggests that high expression of CD41 is a marker for Mk commitment, while CD41 has broader roles in hematopoiesis as highlighted by the fact that CD41$^{-/-}$ mice display multilineage hematopoietic defects (Gekas and Graf, 2013). A recent study reported an increased CD41 expression in HSCs upon aging (Gekas and Graf, 2013). Accordingly, also the expression of other Mk proteins such as CD62P and Vwf increased in the phenotypic HSC compartment upon aging, and treatment of aged mice with pI:C triggered Mk protein synthesis to even higher levels (data not shown). These data are in line with a potential expansion or enhanced maturation of SL-MkPs during aging.

While acute inflammatory signaling drives rapid maturation of MkPs, resulting in increased platelet production, repeated cycles of type-I IFN-mediated inflammation can trigger a constant push of maturation and thus a partial exhaustion of MkPs. These findings reveal that depending on the context and timing, the same inflammatory stimuli can be associated with opposing effects on megakaryopoiesis. This sheds light on the question of why some inflammatory states and diseases are associated with thrombocytosis, whereas others provoke thrombocytopenia

(Cole et al., 1998; Kawamoto, 2003; Martin and Shuman, 1998; Rajan et al., 2005).

EXPERIMENTAL PROCEDURES

In Vivo Treatments

To induce an inflammation, mice were injected intraperitoneal with a single dose of 5 mg/kg pI:C (Invitrogen), 0.25 mg/kg LPS (Sigma), or 0.75 mg/kg recombinant TNFα (PeproTech). Alternatively, mice were treated every third day for 30 days with 5 mg/kg pI:C. Platelet depletion was performed by intravenous injection of 2 mg/kg rat monoclonal antibody directed against mouse GPIb (Emfret Analytics). For transient mTOR blockage, mice were pretreated with 1.5 mg/kg rapamycin 2 hr prior to pI:C treatment.

Transplantation Experiments

For transplantation experiments, $Lin^-cKit^+CD150^+CD48^-CD34^-CD41^{low/med/high}$ HSC populations were FACS-sorted from ACTB-dtTomato mice. 40 HSCs together with 2×10^5 supportive $CD45.2^+$ WT BM were transplanted intrafemorally into lethally irradiated (2 × 500 radiation absorbed dose [rad]) $CD45.2^+$ recipient mice. Peripheral blood was collected at indicated time points and analyzed for $tomato^+$ cells by flow cytometry.

Quantitative Proteomics

Proteomic analysis was performed as described previously (Cabezas-Wallscheid et al., 2014), with minor differences.

H2B-GFP Label-Retention Assays

In vivo label-retention assays using SCL-tTA:H2B-GFP mice were performed as previously described (Wilson et al., 2008). SCL-tTA:H2B-GFP mice were maintained on water containing 2 mg/ml doxycyline hydrate (Sigma) in 5% glucose for a 60 day chase period.

Single-Cell qPCR and Single-Cell RNA-Seq

Single cells were directly sorted into PCR-tubes loaded with lysis buffer using a BD FACSAria II (BD Bioscience) under the single-cell mode. Single-cell qPCR was essentially performed as previously described (Guo et al., 2013), with minor differences. Single-cell RNA-seq was performed according to a modified version of the QUARTZ-Seq protocol (Sasagawa et al., 2013).

Single-Cell Ex Vivo Lineage Tracking

Single-cell ex vivo lineage tracking was performed according to a modified version of the approach described by Eilken et al. (2009).

Electron Microscopy

Transmission electron microscopy was performed as described previously (Platani et al., 2009), with minor differences.

ACCESSION NUMBERS

The proteomics data have been deposited to ProteomeXchange Consortium and are accessible at http://www.ebi.ac.uk/pride with the dataset identifier: PXD001500. The single-cell RNA-seq data can be accessed under Gene Expression Omnibus under accession number GSE64002.

SUPPLEMENTAL INFORMATION

Supplemental Information includes Supplemental Experimental Procedures, six figures, and one table and can be found with this article online at http://dx.doi.org/10.1016/j.stem.2015.07.007.

AUTHOR CONTRIBUTIONS

J.H., D.K., S.H., S.W., A.T., J.K., and M.A.G.E. designed, performed, and/or analyzed proteomics experiments. D.K., J.H., R.S.-M., A.T., and J.K. designed, performed, and/or analyzed electron microscopy experiments. L.V., S.H., K.H., M.A.G.E., and L.M.S. designed, performed, and/or analyzed single-cell RNA-seq experiments. D.L., S.H., M.A.G.E., and T.S. designed, performed, and/or analyzed single-cell ex vivo tracking experiments. S.H., H.U., S.W., A.M.P., A.S., S.B., A.K., M.D.M., and M.A.G.E. designed, performed, and/or analyzed all other in vivo and ex vivo experiments. S.H., J.H., D.K., D.L., L.V., A.M.P., M.D.M., L.M.S., T.S., A.T., J.K., and M.A.G.E. wrote the manuscript.

ACKNOWLEDGMENTS

We would like to thank A. Atzberger and S. Schmitt from the Deutsches Krebsforschungszentrum (DKFZ) Flow Cytometry Facility; D. Krunic from the DKFZ Imaging Core Facility; J. Kirkpatrick, S. Leicht, and K. Dzeyk from the EMBL Proteomics Core Facility; C. Funaya, C. Antony, and Y. Schwab from the EMBL Electron Microscopy Core Facility; members from the EMBL Genomics Core Facility; and the DKFZ Animal Laboratory Services for assistance and their expertise. This work was supported by the BioRN Leading-Edge Cluster "Cell-Based and Molecular Medicine" funded by the German Federal Ministry of Education and Research, the Dietmar Hopp Foundation, and the SFB873 and FOR2033 NicHem, both funded by the Deutsche Forschungsgemeinschaft (DFG).

Received: December 12, 2014
Revised: May 29, 2015
Accepted: July 13, 2015
Published: August 20, 2015

REFERENCES

Baldridge, M.T., King, K.Y., Boles, N.C., Weksberg, D.C., and Goodell, M.A. (2010). Quiescent haematopoietic stem cells are activated by IFN-gamma in response to chronic infection. Nature *465*, 793–797.

Browne, E.P., Wing, B., Coleman, D., and Shenk, T. (2001). Altered cellular mRNA levels in human cytomegalovirus-infected fibroblasts: viral block to the accumulation of antiviral mRNAs. J. Virol. *75*, 12319–12330.

Cabezas-Wallscheid, N., Klimmeck, D., Hansson, J., Lipka, D.B., Reyes, A., Wang, Q., Weichenhan, D., Lier, A., von Paleske, L., Renders, S., et al. (2014). Identification of regulatory networks in HSCs and their immediate progeny via integrated proteome, transcriptome, and DNA methylome analysis. Cell Stem Cell *15*, 507–522.

Cole, J.L., Marzec, U.M., Gunthel, C.J., Karpatkin, S., Worford, L., Sundell, I.B., Lennox, J.L., Nichol, J.L., and Harker, L.A. (1998). Ineffective platelet production in thrombocytopenic human immunodeficiency virus-infected patients. Blood *91*, 3239–3246.

Dorrello, N.V., Peschiaroli, A., Guardavaccaro, D., Colburn, N.H., Sherman, N.E., and Pagano, M. (2006). S6K1- and betaTRCP-mediated degradation of PDCD4 promotes protein translation and cell growth. Science *314*, 467–471.

Eilken, H.M., Nishikawa, S., and Schroeder, T. (2009). Continuous single-cell imaging of blood generation from haemogenic endothelium. Nature *457*, 896–900.

Essers, M.A., Offner, S., Blanco-Bose, W.E., Waibler, Z., Kalinke, U., Duchosal, M.A., and Trumpp, A. (2009). IFNalpha activates dormant haematopoietic stem cells in vivo. Nature *458*, 904–908.

Gekas, C., and Graf, T. (2013). CD41 expression marks myeloid-biased adult hematopoietic stem cells and increases with age. Blood *121*, 4463–4472.

Goerge, T., Ho-Tin-Noe, B., Carbo, C., Benarafa, C., Remold-O'Donnell, E., Zhao, B.Q., Cifuni, S.M., and Wagner, D.D. (2008). Inflammation induces hemorrhage in thrombocytopenia. Blood *111*, 4958–4964.

Guo, G., Luc, S., Marco, E., Lin, T.W., Peng, C., Kerenyi, M.A., Beyaz, S., Kim, W., Xu, J., Das, P.P., et al. (2013). Mapping cellular hierarchy by single-cell analysis of the cell surface repertoire. Cell Stem Cell *13*, 492–505.

Heijnen, H.F., Debili, N., Vainchencker, W., Breton-Gorius, J., Geuze, H.J., and Sixma, J.J. (1998). Multivesicular bodies are an intermediate stage in the formation of platelet alpha-granules. Blood *91*, 2313–2325.

Huang, Z., Richmond, T.D., Muntean, A.G., Barber, D.L., Weiss, M.J., and Crispino, J.D. (2007). STAT1 promotes megakaryopoiesis downstream of GATA-1 in mice. J. Clin. Invest. *117*, 3890–3899.

Ingolia, N.T., Brar, G.A., Rouskin, S., McGeachy, A.M., and Weissman, J.S. (2012). The ribosome profiling strategy for monitoring translation in vivo by deep sequencing of ribosome-protected mRNA fragments. Nat. Protoc. *7*, 1534–1550.

Jenne, C.N., Wong, C.H., Zemp, F.J., McDonald, B., Rahman, M.M., Forsyth, P.A., McFadden, G., and Kubes, P. (2013). Neutrophils recruited to sites of infection protect from virus challenge by releasing neutrophil extracellular traps. Cell Host Microbe *13*, 169–180.

Kawamoto, T. (2003). Use of a new adhesive film for the preparation of multi-purpose fresh-frozen sections from hard tissues, whole-animals, insects and plants. Arch. Histol. Cytol. *66*, 123–143.

Kruiswijk, F., Yuniati, L., Magliozzi, R., Low, T.Y., Lim, R., Bolder, R., Mohammed, S., Proud, C.G., Heck, A.J., Pagano, M., and Guardavaccaro, D. (2012). Coupled activation and degradation of eEF2K regulates protein synthesis in response to genotoxic stress. Sci. Signal. *5*, ra40.

Liu, J., Xu, Y., Stoleru, D., and Salic, A. (2012). Imaging protein synthesis in cells and tissues with an alkyne analog of puromycin. Proc. Natl. Acad. Sci. USA *109*, 413–418.

Machlus, K.R., and Italiano, J.E., Jr. (2013). The incredible journey: From megakaryocyte development to platelet formation. J. Cell Biol. *201*, 785–796.

Månsson, R., Hultquist, A., Luc, S., Yang, L., Anderson, K., Kharazi, S., Al-Hashmi, S., Liuba, K., Thorén, L., Adolfsson, J., et al. (2007). Molecular evidence for hierarchical transcriptional lineage priming in fetal and adult stem cells and multipotent progenitors. Immunity *26*, 407–419.

Martin, T.G., and Shuman, M.A. (1998). Interferon-induced thrombocytopenia: is it time for thrombopoietin. Hepatology *28*, 1430–1432.

Miyamoto, K., Araki, K.Y., Naka, K., Arai, F., Takubo, K., Yamazaki, S., Matsuoka, S., Miyamoto, T., Ito, K., Ohmura, M., et al. (2007). Foxo3a is essential for maintenance of the hematopoietic stem cell pool. Cell Stem Cell *1*, 101–112.

Munsky, B., Neuert, G., and van Oudenaarden, A. (2012). Using gene expression noise to understand gene regulation. Science *336*, 183–187.

Orkin, S.H., and Zon, L.I. (2008). Hematopoiesis: an evolving paradigm for stem cell biology. Cell *132*, 631–644.

Ozbudak, E.M., Thattai, M., Kurtser, I., Grossman, A.D., and van Oudenaarden, A. (2002). Regulation of noise in the expression of a single gene. Nat. Genet. *31*, 69–73.

Platani, M., Santarella-Mellwig, R., Posch, M., Walczak, R., Swedlow, J.R., and Mattaj, I.W. (2009). The Nup107-160 nucleoporin complex promotes mitotic events via control of the localization state of the chromosome passenger complex. Mol. Biol. Cell *20*, 5260–5275.

Platanias, L.C. (2005). Mechanisms of type-I- and type-II-interferon-mediated signalling. Nat. Rev. Immunol. *5*, 375–386.

Rajan, S.K., Espina, B.M., and Liebman, H.A. (2005). Hepatitis C virus-related thrombocytopenia: clinical and laboratory characteristics compared with chronic immune thrombocytopenic purpura. Br. J. Haematol. *129*, 818–824.

Raslova, H., Baccini, V., Loussaief, L., Comba, B., Larghero, J., Debili, N., and Vainchenker, W. (2006). Mammalian target of rapamycin (mTOR) regulates both proliferation of megakaryocyte progenitors and late stages of megakaryocyte differentiation. Blood *107*, 2303–2310.

Sanjuan-Pla, A., Macaulay, I.C., Jensen, C.T., Woll, P.S., Luis, T.C., Mead, A., Moore, S., Carella, C., Matsuoka, S., Bouriez Jones, T., et al. (2013). Platelet-biased stem cells reside at the apex of the haematopoietic stem-cell hierarchy. Nature *502*, 232–236.

Sasagawa, Y., Nikaido, I., Hayashi, T., Danno, H., Uno, K.D., Imai, T., and Ueda, H.R. (2013). Quartz-Seq: a highly reproducible and sensitive single-cell RNA sequencing method, reveals non-genetic gene-expression heterogeneity. Genome Biol. *14*, R31.

Semple, J.W., Italiano, J.E., Jr., and Freedman, J. (2011). Platelets and the immune continuum. Nat. Rev. Immunol. *11*, 264–274.

Shin, J.Y., Hu, W., Naramura, M., and Park, C.Y. (2014). High c-Kit expression identifies hematopoietic stem cells with impaired self-renewal and megakaryocytic bias. J. Exp. Med. *211*, 217–231.

Signer, R.A., Magee, J.A., Salic, A., and Morrison, S.J. (2014). Haematopoietic stem cells require a highly regulated protein synthesis rate. Nature *509*, 49–54.

Stohlawetz, P., Folman, C.C., von dem Borne, A.E., Pernerstorfer, T., Eichler, H.G., Panzer, S., and Jilma, B. (1999). Effects of endotoxemia on thrombopoiesis in men. Thromb. Haemost. *81*, 613–617.

Tacchini-Cottier, F., Vesin, C., Redard, M., Buurman, W., and Piguet, P.F. (1998). Role of TNFR1 and TNFR2 in TNF-induced platelet consumption in mice. J. Immunol. *160*, 6182–6186.

Tothova, Z., and Gilliland, D.G. (2007). FoxO transcription factors and stem cell homeostasis: insights from the hematopoietic system. Cell Stem Cell *1*, 140–152.

Wilson, A., Laurenti, E., Oser, G., van der Wath, R.C., Blanco-Bose, W., Jaworski, M., Offner, S., Dunant, C.F., Eshkind, L., Bockamp, E., et al. (2008). Hematopoietic stem cells reversibly switch from dormancy to self-renewal during homeostasis and repair. Cell *135*, 1118–1129.

Xiang, B., Zhang, G., Guo, L., Li, X.A., Morris, A.J., Daugherty, A., Whiteheart, S.W., Smyth, S.S., and Li, Z. (2013). Platelets protect from septic shock by inhibiting macrophage-dependent inflammation via the cyclooxygenase 1 signalling pathway. Nat. Commun. *4*, 2657.

Yamamoto, R., Morita, Y., Ooehara, J., Hamanaka, S., Onodera, M., Rudolph, K.L., Ema, H., and Nakauchi, H. (2013). Clonal analysis unveils self-renewing lineage-restricted progenitors generated directly from hematopoietic stem cells. Cell *154*, 1112–1126.

Yeaman, M.R. (2014). Platelets: at the nexus of antimicrobial defence. Nat. Rev. Microbiol. *12*, 426–437.